

| | |
|---|---|
| ***Publication Year*** | 2012 |
| ***Acceptance in OA*** | 2022-12-20T15:26:40Z |
| ***Title*** | 3D velocity fields from methanol and water masers in an intermediate-mass protostar |
| ***Authors*** | Goddi, C., MOSCADELLI, Luca, SANNA, ALBERTO |
| ***Publisher's version (DOI)*** | 10.1017/S1743921312007375 |
| ***Handle*** | http://hdl.handle.net/20.500.12386/32789 |
| ***Serie*** | PROCEEDINGS OF THE INTERNATIONAL ASTRONOMICAL UNION |
| ***Volume*** | vol. 8, S287 |

*Cosmic Masers - from OH to $H_0$*
*Proceedings IAU Symposium No. 287, 2012*
*R.S. Booth, E.M.L. Humphreys & W.H.T. Vlemmings, eds.*
© International Astronomical Union 2012
doi:10.1017/S1743921312007375

# 3D velocity fields from methanol and water masers in an intermediate-mass protostar

**C. Goddi[1], L. Moscadelli[2] and A. Sanna[3]**

[1]European Southern Observatory, Karl-Schwarzschild-Strasse 2, D-85748 Garching, Germany
email: cgoddi@eso.org

[2]INAF, Osservatorio Astrofisico di Arcetri, Largo E. Fermi 5, 50125 Firenze, Italy

[3]Max-Planck-Institut für Radioastronomie, Auf dem Hügel 69, 53121 Bonn, Germany

**Abstract.** We report multi-epoch VLBI observations of molecular masers towards the high-mass star forming region AFGL 5142, leading to the determination of the 3D velocity field of circumstellar molecular gas at radii $<0\farcs23$ (or 400 AU) from the protostar MM–1. Our observations of $CH_3OH$ maser emission enabled, for the first time, a direct measurement of infall of a molecular envelope on to an intermediate-mass protostar (radius of 300 AU, velocity of 5 km s$^{-1}$, and infall rate of $6 \times 10^{-4}$ $n_8$ $M_\odot$ yr$^{-1}$, where $n_8$ is the ambient volume density in units of $10^8$ cm$^{-3}$). In addition, our measurements of $H_2O$ maser (and radio continuum) emission revealed a collimated bipolar molecular outflow (and ionized jet) from MM–1. The evidence of simultaneous accretion and outflow at small spatial scales, makes AFGL 5142 an extremely compelling target for high-angular resolution studies of high-mass star formation.

## 1. Introduction

Observational signatures of infalling envelopes and outflowing material in early stages of protostellar evolution, at small radii from the protostar, are essential to further the understanding of the mass-accretion and mass-loss processes, and constrain theoretical models of star formation. To date, bulk infall motions have been detected, mostly by observing inverse P-Cygni profiles of molecular lines (with redshifted absorption and blueshifted emission) along the line-of-sight (l.o.s.) to the infalling gas, against a bright background (dust or H II emission), in both low-mass (e.g., Lee *et al.* 2009) and high-mass (e.g., Beltrán *et al.* 2011) protostars. This method is, however, prone to ambiguous interpretation because line asymmetries may be associated with competing processes such as rotation and outflows, or even arise from superposition of intervening clouds along the l.o.s. Confusion is more severe in the case of high-mass protostars, which are on average more distant (>1 kpc) and form embedded in rich protosclusters. Evidence of infall has been found in only a handful of high-mass star forming regions and on scales of protoclusters rather than individual protostars (>1000 AU: Beltrán *et al.* 2011, and references therein). In order to establish definitely whether the infalling material at large scales eventually accretes on to individual protostars as well as to resolve individual outflows in the protocluster, infall and outflow motions should be measured in the proximity ($\ll$1000 AU) to the protostar.

We report here a convincing signature of infall in a circumstellar molecular envelope with a radius of only 300 AU, associated with the protostar MM–1 in the high-mass star-forming region AFGL 5142 (Zhang *et al.* 2007). MM–1 shows hot-core chemistry (Palau *et al.* 2011), exhibits radio continuum emission from ionized gas, and powers strong water and methanol masers (Goddi *et al.* 2007). Multi-epoch VLBI observations of $CH_3OH$ masers enabled us to measure the 3D velocity field of molecular gas, providing the



https://doi.org/10.1017/S1743921312007375 Published online by Cambridge University Press

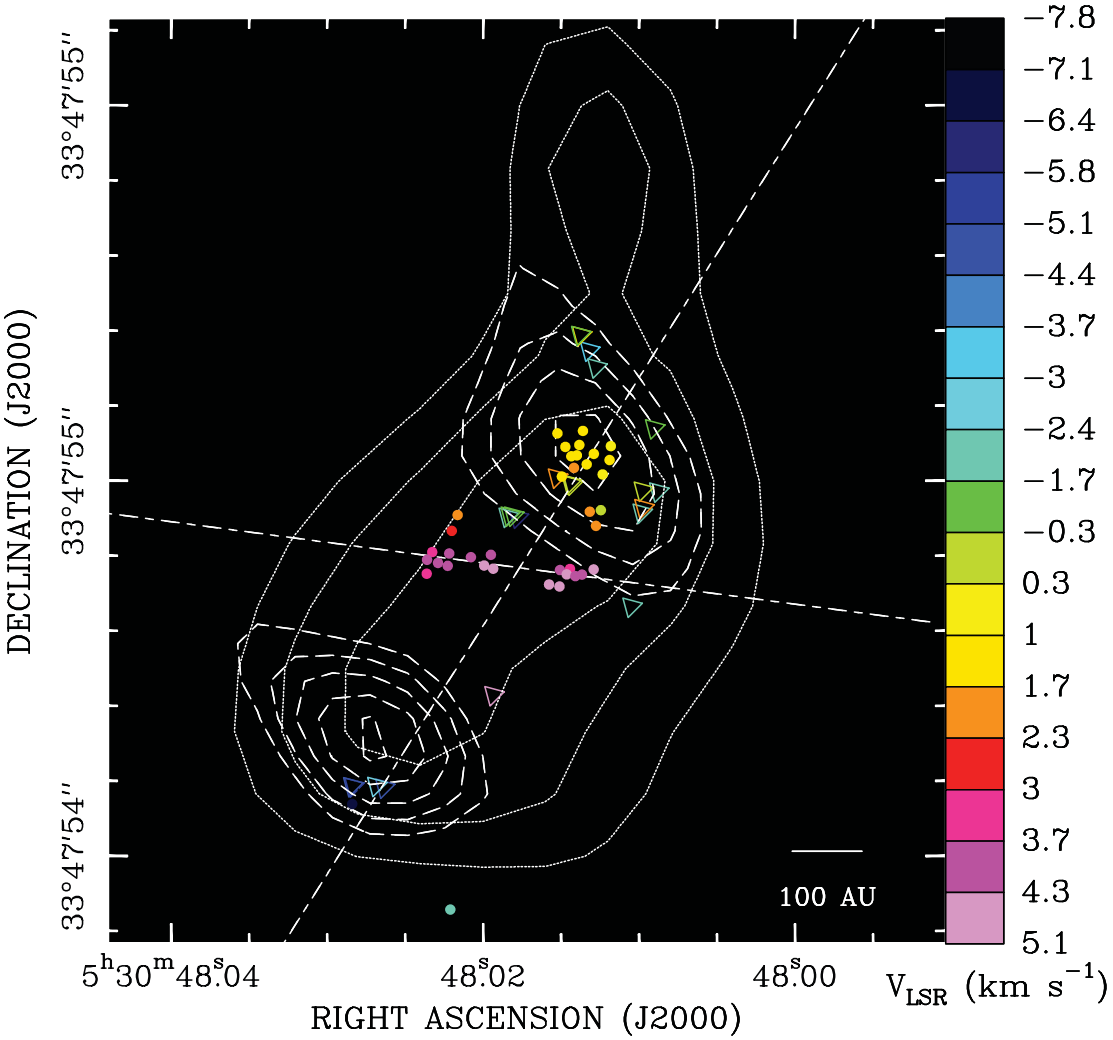


**Figure 1.** Molecular masers and radio continuum in AFGL 5142 MM–1. Positions and l.o.s. velocities of $H_2O$ masers (observed with the VLBA) are indicated by triangles and $CH_3OH$ masers (observed with the EVN) are indicated by circles. Colors code l.o.s. velocities, according to the wedge to the right (the systemic velocity, –1.1 km $s^{-1}$, is in green). The contours show the continuum emissions (observed with the VLA) at 22 GHz (dotted contours, representing 3, 4, and 5 times the 46 $\mu$Jy $beam^{-1}$ rms) and 8.4 GHz (dashed contours, representing 3, 4, 5, 6 and 7 times the 23 $\mu$Jy $beam^{-1}$ rms). The two small-dashed lines show the linear fits to the positions of all water masers (PA –32°) and of only the red methanol masers (PA 82°).

most direct, unbiased measurement, to date, of infall on to an intermediate- to high-mass protostar. We were also able to characterise the outflow structure using the kinematics of $H_2O$ masers and the physical properties of radio continuum emission, thus obtaining a complete picture of star formation on scales <400 AU.

## 2. Observations and Results

We observed the 6.7 GHz $CH_3OH$ masers with the EVN at three distinct epochs (years 2004–2009), the 22.2 GHz $H_2O$ with the VLBA at four distinct epochs (years 2003–2004), and the radio continuum emission with the VLA at 22 GHz and 8.4 GHz. The 3D kinematics of $H_2O$ and $CH_3OH$ masers is discussed in detail in Goddi *et al.* (2006, 2007, 2011). Figure 1 shows positions and l.o.s. velocities of the 22 GHz water and the 6.7 GHz methanol masers, overplotted on the contour maps of the continuum emission at 8.4 GHz and 22 GHz. The 22 GHz continuum emission (0.″24 beamwidth) appears elongated NW-SE, while the 8.4 GHz emission (0.″16 beamwidth) is resolved into

https://doi.org/10.1017/S1743921312007375 Published online by Cambridge University Press

two components separated by 300 mas (or 540 AU) on the plane of the sky. $H_2O$ masers are concentrated in two clusters, associated with the two components of the 8.4 GHz continuum: that towards the SE has l.o.s. velocities blue-shifted with respect to the systemic velocity of the region (–1.1 km s$^{-1}$; Zhang *et al.* 2007); the second, located to the NW has red-shifted l.o.s. velocities. $CH_3OH$ masers are distributed across an area similar to the $H_2O$ masers, and consist mainly of two clusters: one with moderately red-shifted l.o.s. velocities is associated with the NW continuum peak ("yellow" features); the other cluster with the most red-shifted l.o.s. velocities lies in between the two 8.4 GHz peaks ("red" features). The dashed lines in Fig. 1 provide the best (least-squares fit) to the positions of all the water masers (position angle or PA of –32°) and to only the red methanol masers (PA of 82°), respectively.

Figure 2 shows the proper motions of $H_2O$ masers (left panel) and $CH_3OH$ masers (right panel). Since measurements of *absolute* proper motions are affected by the combined uncertainty of the Solar motion and Galactic rotation curve (up to 15 km s$^{-1}$; Reid *et al.* 2009), we prefer to base our analysis on *relative* velocities for both water and methanol masers. This requires us to adopt a suitable reference frame, ideally centered on the protostar. For water, we calculated the geometric mean of positions at individual epochs, for all the masers persistent over four epochs (hereafter "center of motion") and we referred the proper motions to this point (this is equivalent to subtracting from all masers, the average proper motion of the selected features). The proper motions indicate that the two clusters are moving away from each other, NW-SE, with velocities ∼15 km s$^{-1}$. We used positions and 3D velocities of water masers to define geometric parameters of the outflow (for simplicity, supposed of conical shape): PA of the sky-projected axis (–40°), inclination angle of the axis with the plane of the sky (25°), and opening angle (25°).

Since the amplitude of methanol proper motions is much lower than that of water (with mean values ∼3 km s$^{-1}$ and ∼15 km s$^{-1}$, respectively), the choice of a suitable reference for methanol velocities is more critical. The red masers have *internal* proper motions (calculated using the center of motion of only red masers; 1–2 km s$^{-1}$) much smaller than the internal proper motions of the yellow masers (relative to the center of motion of only yellow features; 1–10 km s$^{-1}$); the opposite is true for their l.o.s. velocities (3–6 km s$^{-1}$ vs. 0–2 km s$^{-1}$). Since red masers are projected in the plane of the sky closer to the protostellar position and move mostly along the l.o.s., we assume that their average proper motion gives an estimate of the protostar proper motion. Hence, we calculated the center of motion of methanol using only red features with a stable spatial and spectral structure. The resulting proper motions (Fig. 2, right), should represent the sky-projected velocities as measured by an observer co-moving with the star. The yellow masers have proper motions with larger amplitudes, directed towards the the red maser centroid, which instead move mostly along the l.o.s.; both aspects indicate infall towards the protostar.

## 3. Discussion

Our VLBI observations show that water and methanol masers, despite being excited at similar radii from MM–1, trace different kinematics: outflow and infall, respectively.

*Collimated outflow from MM–1.* We have identified a collimated bipolar outflow, at radii 140 to 400 AU from the driving protostar, traced by radio continuum emission in its ionized component and by water masers in its molecular component. For optically thin emission, $F\,d^2 = 10^{3.5}\,(\Omega/4\pi)\,\dot{P}_{jet}$ (Sanna *et al.* 2010), where $F$ is the continuum flux density in mJy, $\dot{P}_{jet}$ is the jet momentum rate in $M_\odot$ yr$^{-1}$ km s$^{-1}$, $\Omega$ is the jet solid angle in

https://doi.org/10.1017/S1743921312007375 Published online by Cambridge University Press

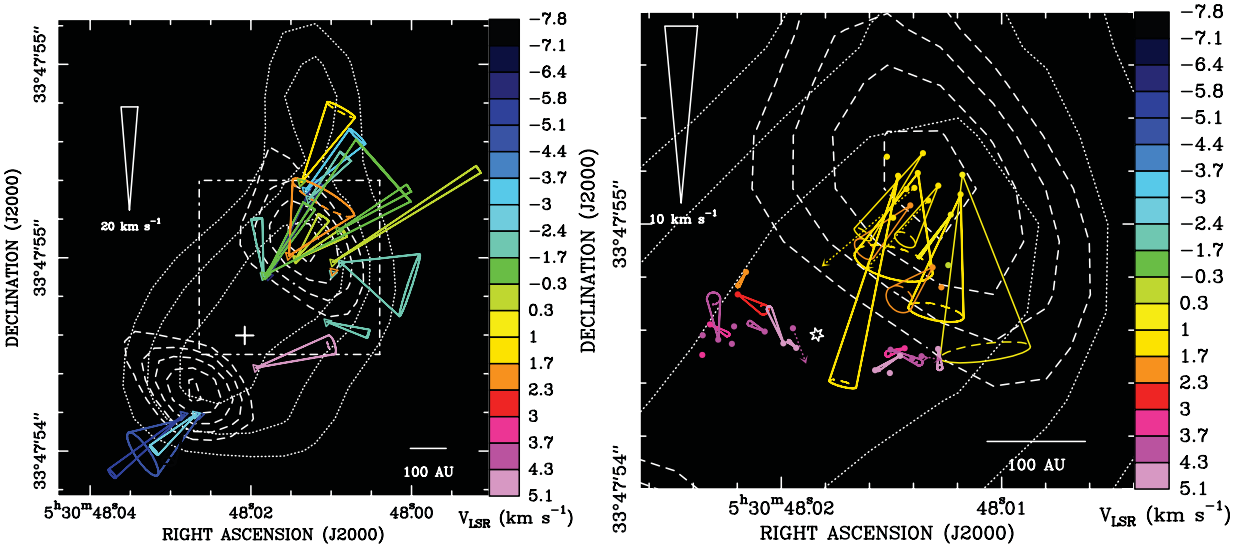


**Figure 2.** Proper motions of $H_2O$ (*left panel*) and $CH_3OH$ (*right panel*) masers in AFGL 5142 MM–1, as measured relative to their centers of motion, independently calculated for water (*cross*) and methanol (*star*). The rectangle in the left panel shows the area plotted in the right panel. The cones indicate orientation and uncertainties of measured proper motions (the amplitude scale is given in each panel) and colors denote l.o.s. velocities. Contour maps show the VLA 22 GHz (dotted line) and 8.4 GHz (dashed line) continuum.

sr, and $d$ is the source distance in kpc. For $d$ =1.8 kpc and $F$=0.24 (0.17) mJy for the NW (SE) component at 8.4 GHz, we derive: $\dot{P}_{jet} = 2.5(1.7)\times10^{-4}\ (\Omega/4\pi)^{-1}\ M_\odot\ \mathrm{yr}^{-1}\ \mathrm{km\ s}^{-1}$. Based on our measurements of positions and 3D velocities of water masers and under reasonable assumptions for gas densities, we can estimate the mass-loss rate, $\dot{M}_{out} = 4\pi R^2 n_{H_2} m_{H_2} V\ (\Omega/4\pi)$, and the momentum rate, $\dot{P}_{out}=\dot{M}_{out}V$, of the molecular outflow. For an average projected distance of water masers from the protostar of 290 AU and an average velocity of 15 km s$^{-1}$, we derive $\dot{M}_{out} = 1.9\times10^{-3}\ (\Omega/4\pi)\ n_8\ M_\odot\ \mathrm{yr}^{-1}$, where $\Omega$ is the (conical) flow solid angle and $n_8$ is the ambient volume density in units of $10^8$ cm$^{-3}$. If the water masers originate in shocks produced by the interaction of the ionized jet with the ambient medium, then $\Omega$ can be determined by requiring that the momentum rate in the maser outflow equals that from the continuum emission. We derive $\Omega$=1–1.2 sr, corresponding to an outflow semi-opening angle of 32–36°, which provides $\dot{M}_{out} = 1.6\times10^{-4}\ n_8\ M_\odot\ \mathrm{yr}^{-1}$ and $\dot{P}_{out} = 2.4\times10^{-3}\ n_8\ M_\odot\ \mathrm{yr}^{-1}\ \mathrm{km\ s}^{-1}$, indicating strong outflow activity from MM–1.

*Gas infall on to MM–1 from a molecular envelope.* Infall onto MM–1 was first claimed by Goddi *et al.* (2007), based solely on positions and l.o.s. velocities of methanol masers. The measurement of proper motions has provided the missing kinematic observable to confirm the infall hypothesis.

We adopted a simple spherical model: $\mathbf{V}(\mathbf{R}) = (2\ G\ M/R^3)^{1/2}\ \mathbf{R}$, where $\mathbf{V}$ is the velocity field, $\mathbf{R}$ is the position vector from the protostar, $M$ is the total gas mass within a sphere of radius $R$ centered on the protostar. The best-fit parameters we derived from the model are: $R$=290 AU and $M$=4 $M_\odot$, corresponding to $V_{\rm inf}$=5 km s$^{-1}$. Figure 3 shows the measured and best-fit model 3D velocity vectors of methanol masers projected onto the plane containing the protostar and perpendicular to the outflow axis (the equatorial plane; left panel) and the plane containing the l.o.s. and the outflow axis (right panel). Most of the measured 3D velocities are well reproduced by the infall model. The two projections show also that methanol masers do not sample the whole spherical envelope but concentrate into preferred areas. We interpret this behavior in terms of amplification of a background emission. The yellow features lie on top of the NW 8.4 GHz continuum peak,

https://doi.org/10.1017/S1743921312007375 Published online by Cambridge University Press

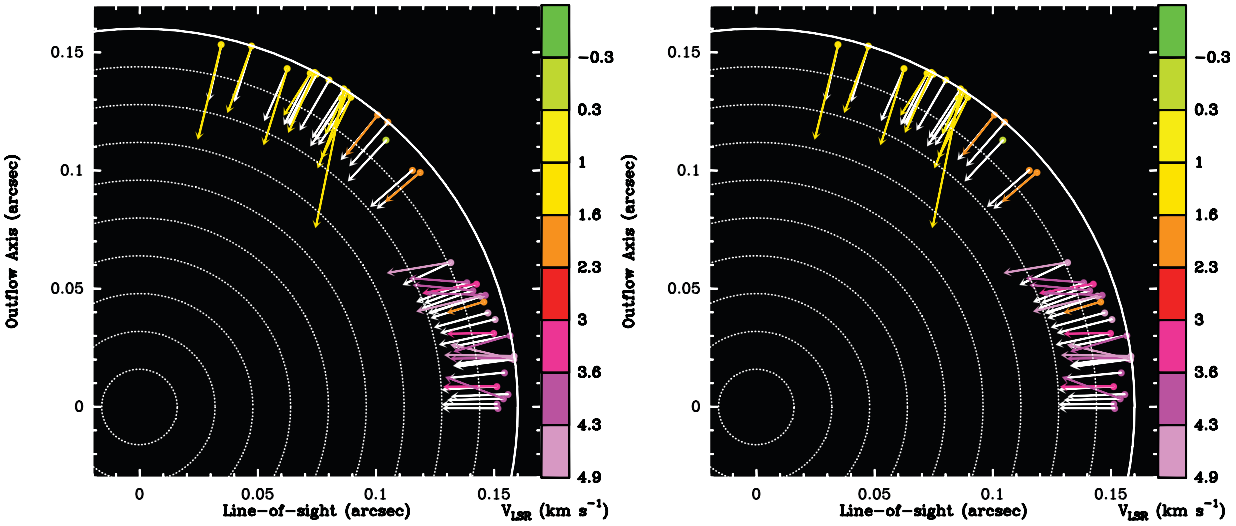


**Figure 3.** Measured (*color arrows*) and best-fit model (*black arrows*) 3D velocity vectors of $CH_3OH$ masers. We show projections onto the equatorial plane of the envelope (*left panel*) and a plane containing the l.o.s. and the outflow axis (*right panel*). We assume an edge-on equatorial plane. The dotted lines indicate concentric circles at steps of 10% of the envelope radius (0.″16) around the protostar at the (0,0) position.

which naturally provides the background radiation being amplified. The red features are projected closer to the protostellar position and background source may be a compact HII region and/or an ionized wind with a size smaller than the extent of methanol masers (0.″14). Alternately, the elongation of red features could be explained by the larger densities expected in the equatorial plane (a disk?), providing longer amplification path for the maser radiation.

We can now use the best-fit parameters for the sphere radius and infall velocity derived from our model, to estimate a mass infall rate, $\dot{M}_{\rm inf} = 4\pi R^2 n_{H_2} m_{H_2} V_{\rm inf}$, and an infall momentum rate, $\dot{P}_{\rm inf} = \dot{M}_{\rm inf} V_{\rm inf}$. For $R = 290$ AU and $V_{\rm inf} = 5$ km s$^{-1}$, we obtain: $\dot{M}_{\rm inf} = 6\times10^{-4}\ n_8\ M_\odot$ yr$^{-1}$ and $\dot{P}_{\rm inf} = 3\times10^{-3}\ n_8\ M_\odot$ km s$^{-1}$ yr$^{-1}$. On the one hand, the high infall rate might indicate that the protostar is actively accreting. On the other hand, a ratio of 0.27 for the mass-loss to the infall rate indicates that the outflow can efficiently remove mass (and angular momentum) from the system, as expected from magneto-centrifugal ejection. We caution however that the estimated mass rates are accurate only to within 1–2 orders of magnitude, owing to the wide range of densities required for maser excitation (Kaufman & Neufeld 1996; Cragg *et al.* 2005). Nevertheless, our measurements show that the two maser species used to derive the mass-loss ($H_2O$) and the mass-infall ($CH_3OH$) rates are distributed across a similar area, making plausible the hypothesis that they may be excited in molecular gas with similar densities, ($10^8$ cm$^{-3}$). Hence, the dependence of the outflow/infall rate ratio on gas density should be less critical.

We estimated 4 $M_\odot$ gas mass for the infalling envelope, consistent with the value estimated from dust continuum emission (3 $M_\odot$; Zhang *et al.* 2007). Hence, AFGL 5142 MM–1 may be the lowest mass protostar known to be associated with Class II methanol masers. We argue that accretion onto a 4 $M_\odot$ protostar may explain the bolometric luminosity of the region and possibly provide the strong IR background to pump the methanol masers. We define the accretion luminosity as $L_{\rm acc} = G\dot{M}_{\rm inf} M_*/R_*$ , where $\dot{M}_{\rm inf}$ is the mass infall rate, and $M_*$ and $R_*$ are the mass and radius of the protostar. Our infall model provides an estimate for $\dot{M}_{\rm inf}$ and $M_*$, while $R_*$ can be derived from the mass-radius relation in protostellar models: $R_* = 8\ R_\odot$ for $M_* = 4\ M_\odot$ and $\dot{M}_{\rm inf} = 10^4\ M_\odot$ yr$^{-1}$ (Palla & Stahler 1993). We then derive: $L_{\rm acc} \sim 10^4\ n_8\ L_\odot$, comparable with the bolometric luminosity of the region (Zhang *et al.* 2007). Alternatively, our analysis

https://doi.org/10.1017/S1743921312007375 Published online by Cambridge University Press

may provide only a lower limit to the protostellar mass, as suggested by the powerful outflow activity, evidenced by strong water maser and radio continuum emission, and the large mass of the CO outflow (3 $M_{\odot}$). In fact, our infall model considers only gravity but likely non-gravitational (e.g., centrifugal and magnetic) forces can influence gas dynamics and possibly lead to underestimates of the central object mass. Future interferometric observations of thermal dense gas tracers at sub-arcsecond resolution (with ALMA) may help to resolve the accretion disk around MM–1 and to derive a rotation curve, which would give a robust estimate of the protostellar mass.

## References

Beltrán, M. T., Cesaroni, R., Neri, R., & Codella, C. 2011, *A&A*, 525, A151
Cragg, D. M., Sobolev, A. M., & Godfrey, P. D. 2005, *MNRAS*, 360, 533
Goddi, C. & Moscadelli, L. 2006, *A&A*, 447, 577
Goddi, C., Moscadelli, L., Sanna, A., Cesaroni, R., & Minier, V. 2007, *A&A*, 461, 1027
Goddi, C., Moscadelli, L., & Sanna, A. 2011, *A&A* (Letters), 535, L8
Kaufman, M. J. & Neufeld, D. A. 1996, *ApJ*, 456, 250
Lee, C.-F., Mao, Y.-Y., & Reipurth, B. 2009, *ApJ*, 694, 1395
Palau, A., Fuente, A., Girart, J. M., *et al.* 2011, *ApJ* (Letters), 743, L32
Palla, F. & Stahler, S. W. 1993, *ApJ*, 418, 414
Reid, M. J., Menten, K. M., Zheng, X. W., *et al.* 2009, *ApJ*, 700, 137
Sanna, A., Moscadelli, L., Cesaroni, R., *et al.* 2010, *A&A*, 517, A71
Zhang, Q., Hunter, T. R., Beuther, H., *et al.* 2007, *ApJ*, 658, 1152

https://doi.org/10.1017/S1743921312007375 Published online by Cambridge University Press